PHYSICAL REVIEW C VOLUME 9, NUMBER 2 FEBRUARY 1974

Theory of final-state interactions in three-particle systems*

R. T. Cahill
School of Physical Sciences, The Flinders University of South Australia, Bedford Park, Australia 5042
(Received 12 April 1973; revised manuscript received 10 September 1973)

The form, as determined by the coherence formalism, of the final-state-interaction (fsi) amplitude for three-particle breakup reactions is derived from the Faddeev equations in the case of n-d breakup. A parametrization of the Faddeev amplitudes in the fsi region is presented and interpreted. The detailed analytic form of fsi differential cross sections is obtained, showing that the most important fsi parameters are the two-particle scattering length and an effective target size, which exhibits dilation effects. Analysis of experiments with the theory implies charge symmetry of nuclear forces.

[NUCLEAR REACTIONS $n(d,nn)p$; final-state-interaction theory. Coherence formalism, Faddeev-amplitude parametrization, initial-state interaction.]

I. INTRODUCTION

In three-particle scattering theory the understanding of final-state interactions in breakup reactions of the type $1+(2,3)\rightarrow 1+2+3$ is an important problem. In particular we are interested in knowing how the information about a given pair's interaction is distributed over the entire amplitude and hence in the differential cross sections. The particular example we shall use to illustrate the general theory is the breakup reaction $n+d\rightarrow p+n+n$, for which the n-n pair interaction is of special interest, particularly the n-n scattering length a_{nn}. Previous analyses of this reaction were, in most cases, based on extreme and unjustified approximations, which essentially involved using only low-order multiple-scattering diagrams. The resulting extracted values for a_{nn} had a large and inconsistent spread, making it difficult to finally resolve the question of charge symmetry or charge independence of nucleon-nucleon forces.

In this paper we present a detailed analysis of the Faddeev scattering equations in the final-state-interaction regions of the n-d breakup reaction. In Sec. II we derive the general structure of the final-state-interaction (fsi) amplitude. This analysis reveals the form and importance of the coherence between different types of scattering processes, namely those that involve, say, n-n rescattering and those that do not. This coherence effect is of paramount importance in understanding and analyzing fsi in kinematically incomplete experiments. The coherence formalism achieves an additional simplification. The usual description for calculating the fsi peak shape, say in the proton energy spectrum from n-d breakup, involves an integration, over final states, of a linear combination of various component amplitudes, which are solutions of the Faddeev equations. The exact coherence formalism, however, expresses the fsi amplitude in terms of only one component amplitude. Knowing the analytic form of this component amplitude, which we determine in Sec. III, we then obtain in Sec. IV the detailed but simple structure of the fsi cross section for single-particle energy spectra. Because we have performed a complete analysis, the spectra calculated with this theory agree completely with those obtained directly from the Faddeev equations.

The results show how, say, the n-n scattering phase shift appears in the cross section. It also shows that of the three-particle parameters which enter into the cross section, the most important is one that is effectively a measure of the deuteron size, and that furthermore the value of this parameter, when determined and compared from both low-order multiple-scattering amplitudes and the exact numerical solutions of the Faddeev equations, shows an apparent deuteron dilation effect in the exact solution. This dilation strongly influences the width of the fsi peak.

The general form of the fsi peak resolves a number of puzzles—namely why the simple Watson-Migdal fsi theory fails in kinematically incomplete experiments and why analyses with this theory favor charge independence. As well we determine criteria for the use of the Watson-Migdal theory in both kinematically complete and incomplete experiments. As a simple application of the new fsi theory we reanalyze, approximately, some earlier experimental proton spectra from n-d breakup which when previously analyzed with the Watson-Migdal theory gave obviously erroneous results. For example, the extracted value for a_{nn}, which if anything implied charge independence, depended strongly on the three-particle energy of the exper-

iment. The new fsi theory gives a charge symmetry value for a_{nn} of -17 fm from this experiment and shows that the energy dependence of a_{nn} in the Watson-Migdal-type analysis can easily be interpreted as due to the energy dependence of the deuteron dilation effect.

We present evidence that this deuteron dilation effect can be understood in terms of the strong n-d initial-state interaction. The parameter which measures the apparent deuteron dilation can be measured in the proton energy spectrum in the n-n fsi region and from the quasifree scattering peak width. It would seem particularly worthwhile to perform such experiments in order to systematically study this effect.

We also show that the very strong influence of the coherence effect on fsi in n-d breakup depends very much on the sign of the scattering length of the pair interaction involved in the fsi. The experimental results then imply that a_{nn} is negative, which could not be determined from the Watson-Migdal-type analysis.

II. COHERENCE FORMALISM

The Faddeev equations,[1] for the breakup reaction n-$d \to n+n+p$ with S-wave spin-dependent and charge-dependent nucleon-nucleon scattering amplitudes, become[2,3] coupled integral equations for component amplitudes

$$N_n^{(S)}(\vec{k}',q';\vec{k}) = \chi_{n1}^{(S)}\langle q'|t_n\left(E-\frac{3}{4}\frac{\hbar^2}{m}k'^2+i\epsilon\right)|\tfrac{1}{2}\vec{k}'+\vec{k}\rangle\phi(\vec{k}'+\tfrac{1}{2}\vec{k})$$

$$+\sum_{n'=1}^{n_S}\chi_{nn'}^{(S)}\int d^3k''\frac{\langle q'|t_n\left(E-\frac{3}{4}\frac{\hbar^2}{m}k'^2+i\epsilon\right)|\frac{1}{2}\vec{k}'+\vec{k}''\rangle}{E-\frac{\hbar^2}{m}(k'^2+k''^2+\vec{k}'\cdot\vec{k}'')+i\epsilon}N_{n'}^{(S)}(\vec{k}'',|\vec{k}'+\tfrac{1}{2}\vec{k}''|;\vec{k}), \tag{2.1}$$

where E is the total energy, $\vec{k}$ the incident momentum, $\vec{k}'$ is the momentum of one nucleon, and $\vec{q}'$ is the relative momentum of the remaining pair. The deuteron wave function is ϕ and $\langle q|t_n(e)|p\rangle$ is the off-shell S-wave nucleun-nucleon scattering matrix where $n=1$ denotes the $^3S_1$ n-p interaction, $n=2$ the $^1S_0$ n-p interaction, and $n=3$ the $^1S_0$ n-n interaction. The three-nucleon spin is $S=\frac{1}{2}$ (doublet-state D) and $S=\frac{3}{2}$ (quartet-state Q). We have one coupled equation in the quartet-spin channel ($n_{3/2}=1$) and three in the doublet-spin channel ($n_{1/2}=3$). The various coupling constants $\chi_{nn'}^{(1/2)}$ can be displayed as a matrix

$$\chi^{(1/2)}=\begin{pmatrix} \frac{1}{2} & -\frac{1}{2} & -1 \\ -\frac{3}{2} & -\frac{1}{2} & 1 \\ -\frac{3}{2} & \frac{1}{2} & 0 \end{pmatrix},$$

while for the quartet-spin state there is only one coefficient $\chi_{11}^{(3/2)}=-1$.

The four amplitudes $N_n^{(S)}(\vec{k}',q';\vec{k})$ are easily interpreted. For example, $N_3^{(1/2)}$ sums all multiple scatterings which end in n-n rescattering. The three remaining component amplitudes account for n-p final rescattering in various spin states.

The various cross sections are determined by

$$|M|^2=\tfrac{2}{3}|M_Q|^2+\tfrac{1}{3}|M_{D1}|^2+\tfrac{1}{3}|M_{D2}|^2,$$

where the quartet-spin amplitude is

$$M_Q(\vec{k}_1,\vec{q}_1;\vec{k})=N_1^{(3/2)}(\vec{k}_2,q_2;\vec{k})-N_1^{(3/2)}(\vec{k}_3,q_3;\vec{k}), \tag{2.2}$$

and for the two doublet-spin amplitudes

$$M_{D_1}(\vec{k}\vec{q}_t\ ;\vec{k})=\tfrac{1}{2}[N_1^{(1/2)}(\vec{k}_2,q_2;\vec{k})-N_1^{(1/2)}(\vec{k}_3,q_3;\vec{k})]$$
$$+\tfrac{1}{2}[N_2^{(1/2)}(\vec{k}_2,q_2;\vec{k})-N_2^{(1/2)}(\vec{k}_3,q_3;\vec{k})], \tag{2.3}$$

and

$$M_{D_2}(\vec{k}_1,\vec{q}_1;\vec{k})=\frac{1}{2\sqrt{3}}[N_2^{(1/2)}(\vec{k}_2,q_2;\vec{k})+N_2^{(1/2)}(\vec{k}_3,q_3;\vec{k})]$$
$$-\frac{\sqrt{3}}{2}[N_1^{(1/2)}(\vec{k}_2,q_2;\vec{k})+N_1^{(1/2)}(\vec{k}_3,q_3;\vec{k})]$$
$$+\frac{2}{\sqrt{3}}N_3^{(1/2)}(\vec{k}_1,q_1;\vec{k}). \tag{2.4}$$

Here $\vec{k}_1$ is the proton barycentric momentum in the final state and $\vec{q}_1$ is the n-n relative momentum, while $\vec{k}_2$ and $\vec{k}_3$ are the neutron momenta,

$$\vec{k}_2=\vec{q}_1-\tfrac{1}{2}\vec{k}_1$$

and

$$\vec{k}_3=-\vec{q}_1-\tfrac{1}{2}\vec{k}_1,$$

and the n-p relative momenta are

$$\vec{q}_2=-\tfrac{1}{2}\vec{q}_1-\tfrac{3}{4}\vec{k}_1$$

and

$$\vec{q}_3=-\tfrac{1}{2}\vec{q}_1+\tfrac{3}{4}\vec{k}_1.$$

The laboratory-system proton differential energy

spectrum is

$$\frac{d\sigma}{dE_p d\Omega_p} = (2\pi)^4 \frac{k_p q_1}{6k}\left(\frac{m}{\hbar^2}\right)^3 \int d\hat{q}_1 |M|^2 , \qquad (2.5)$$

where k_p is the proton laboratory momentum. The corresponding neutron differential energy spectrum is given by

$$\frac{d\sigma}{dE_n d\Omega_n} = (2\pi)^4 \frac{k_n q_2}{6k}\left(\frac{m}{\hbar^2}\right)^3 \int d\hat{q}_2 |M|^2 . \qquad (2.6)$$

We first consider the high-energy end of the proton spectrum, from Eq. (2.5), which is dominated by the large narrow n-n fsi peak (curve 1 of Fig. 5). In this region M_Q and M_{D_1} are very small due to the n-n antisymmetrization evident in Eqs. (2.2) and (2.3), and M_{D_2} is responsible for the n-n fsi peak. Furthermore it might be expected that the component amplitude $N_3^{(1/2)}$, in M_{D_2} in Eq. (2.4), corresponding to final n-n rescattering is responsible for the n-n fsi peak, with the peak perhaps broadened by interference between $N_3^{(1/2)}$ and the remaining four terms in Eq. (2.4). However, on the contrary, numerical calculations[2,3] have shown that the linear combination in M_{D_2} produces a much narrower fsi peak than does $N_3^{(1/2)}$ alone (curve 4 of Fig. 5). Thus this linear combination is coherent, with the sum producing a narrower peak than any individual term in the sum. Hence the n-n interaction information is distributed over the five amplitudes in Eq. (2.4). It is important to understand the mechanism of this coherence effect since, for example, any approximate three-particle scattering theories will most likely not preserve the coherence. This coherence effect has been examined in general terms by Amado[4] who considered the Faddeev operator integral equations and concluded that the coherent linear combination carries the phase factor $e^{i\delta(s)}$, and by Aitchison and Kacser[5] using a simple dispersion theory. The actual structure of the coherence mechanism has been given by Cahill[6] from analysis of the Faddeev equations for the three identical boson system.

We now derive the coherence mechanism for the n-n fsi in n-d breakup and show how this leads to an understanding of how the n-n scattering information is contained in the fsi peak structure.

Introduce the n-n relative angular momentum decomposition for the on-shell three-particle amplitude ($\frac{3}{4}k_i^2 + q_i^2 = mE/\hbar^2$ on shell),

$$M_{D_2}(\vec{k}_1, \vec{q}_1; \vec{k}) = \sum_{lm} M_{D_2}^{(lm)}(q_1, z_1) Y_l^m(\hat{q}_1) ,$$

where $z_1 = \hat{k}_1 \cdot \hat{k}$. The differential cross section in Eq. (2.5) becomes

$$\frac{d\sigma}{dE_p d\Omega_p} = \tfrac{1}{3} P(E_p) |M_{D_2}^{(00)}(q_1, z_1)|^2 + P(E_p) B_{nn}(q_1, z_1) , \qquad (2.7)$$

where $P(E_p)$ is the phase-space factor in Eq. (2.5). Here

$$B_{nn}(q_1, z_1) = \tfrac{1}{3} \sum_{lm, l\neq 0} |M_{D_2}^{(lm)}(q_1, z_1)|^2 + \int d\hat{q}_1 (\tfrac{2}{3}|M_Q|^2 + \tfrac{1}{3}|M_{D_1}|^2). \qquad (2.8)$$

From the antisymmetry of M_Q and M_{D_1} and since the sum in Eq. (2.8) excludes $l=0$ we see that $B_{nn}(q_1, z_1)$ is zero when $q_1 = 0$, that is, when the proton energy E_p is a maximum, and that in the n-n fsi region $B_{nn}(q_1, z_1)$ is small. The contribution $P(E_p)$ $B_{nn}(q_1, z_1)$ to the cross section is shown by curve 2 in Fig. 5. Hence this term acts as an incoherent background to the n-n peak, and the peak arises solely from $M_{D_2}^{(00)}(q_1, z_1)$, which is consistent with the n-n fsi being in the n-n S-wave state only.

We define [where $s_i = (\hbar^2/m)q_i^2$ are final-state relative subenergies]

$$F_3^{(1/2)}(s_1, z_1) = \frac{\sqrt{3}}{2}\frac{1}{(4\pi)^{1/2}} M_{D_2}^{(00)}(q_1, z_1)$$

to be the n-n coherent fsi amplitude, where from Eq. (2.4),

$$F_3^{(1/2)}(s_1, z_1) = N_3^{(1/2)}(\vec{k}_1, q_1; \vec{k}) + \frac{1}{8\pi}\int d\hat{q}_1 N_2^{(1/2)}(\vec{q}_1 - \tfrac{1}{2}\vec{k}_1, |\tfrac{1}{2}\vec{q}_1 + \tfrac{3}{4}\vec{k}_1|; \vec{k}) - \frac{3}{8\pi}\int d\hat{q}_1 N_1^{(1/2)}(\vec{q}_1 - \tfrac{1}{2}\vec{k}_1, |\tfrac{1}{2}\vec{q}_1 + \tfrac{3}{4}\vec{k}_1|; \vec{k}), \qquad (2.9)$$

which is the coherent part of M_{D_2}. To exhibit the coherence we now use the fact that the three amplitudes in Eq. (2.9) are related by the coupled integral equations of Eq. (2.1).

For a half-off-shell two-particle scattering matrix we have in general[7,4] (for any particular partial wave, here S wave),

$$\langle q_i | t_n(s_i) | p \rangle = \langle q_i | t_n(s_i) | q_i \rangle A_n(q_i, p) = -\frac{\hbar^2}{2m\pi^2} f_n(s_i) A_n(q_i, p) ,$$

where clearly $A_n(q, q) = 1$. The nucleon-nucleon scattering amplitude $f_n(s)$ is, in terms of the phase shift $\delta_n(s)$,

$$f_n(s) = \frac{e^{i\delta_n(s)} \sin\delta_n(s)}{q} .$$

Putting $\vec{k}'$ and $\vec{q}'$ on shell and changing the integration variable to $\vec{q}'' = \frac{1}{2}\vec{k}' + \vec{k}''$, Eq. (2.1) gives that the on-shell component amplitudes have the form

$$N_n^{(S)}(q', z) = f_n(s') R_n^{(S)}(s', z), \tag{2.10}$$

where

$$R_n^{(S)}(s', z) = -\frac{\hbar^2}{2\pi^2 m}\chi_{n1}^{(S)} A_n(q', |\tfrac{1}{2}\vec{k}' + \vec{k}|)\,\phi(\vec{k}' + \tfrac{1}{2}\vec{k})$$
$$-\frac{1}{2\pi^2}\sum_{n'=1}^{n_S}\chi_{nn'}^{(S)}\int d^3q''\,\frac{A_n(q', q'')}{q'^2 - q''^2 + i\epsilon}$$
$$\times N_{n'}^{(S)}(\vec{q}'' - \tfrac{1}{2}\vec{k}_1, |\tfrac{1}{2}\vec{q}_1 + \tfrac{3}{4}\vec{k}'|; \vec{k}),$$

and we see that $R_n^{(S)}(s, z)$ has a square-root branch point at $s = 0$ due to the propagator, with the following discontinuity across the branch cut [in k' this branch point is at $(\frac{4}{3}mE/\hbar^2)^{1/2}$]:

$$\Delta R_n^{(S)}(s', z)$$
$$= \frac{iq'}{2\pi}\sum_{n'=1}^{n_S}\chi_{nn'}^{(S)}\int d\hat{q}'\, N_{n'}^{(S)}(\vec{q}' - \tfrac{1}{2}\vec{k}', |\tfrac{1}{2}\vec{q}' + \tfrac{3}{4}\vec{k}'|; \vec{k}). \tag{2.11}$$

Using Eqs. (2.10) and (2.11) and the values for $\chi_{nn'}^{(1/2)}$, Eq. (2.9) becomes

$$F_3^{(1/2)}(s_1, z_1) = \frac{e^{i\delta_3(s_1)}}{2iq_1}$$
$$\times \Delta[e^{i\delta_3(s_1)} R_3^{(1/2)}(s_1, z_1)], \tag{2.12}$$

where $\Delta[\cdots]$ denotes a branch-cut discontinuity. Equation (2.12) is the basic expression of the coherence effect for the n-n fsi. We see that while the n-n rescattering term, $N_3^{(1/2)}$ in Eq. (2.4), by itself does not describe the n-n fsi, since the five terms in Eq. (2.4) are coherent, the $N_3^{(1/2)}$ amplitude nevertheless does contain all the fsi information, as shown by Eqs. (2.10) and (2.12). Equation (2.12) involves however both the "physical" amplitude $R_3^{(1/2)}(s + i\epsilon, z)$ and the "unphysical" amplitude $R_3^{(1/2)}(s - i\epsilon, z)$. The full coherent n-n fsi part of the proton energy spectrum has the form

$$\left[\frac{d\sigma}{dE_p d\Omega_p}\right]_{\text{fsi}} = \frac{4\pi}{9}\frac{P(E_p)}{q_1^2}$$
$$\times |\Delta[e^{i\delta_3(s_1)} R_3^{(1/2)}(s_1, z_1)]|^2, \tag{2.13}$$

whereas the n-n rescattering amplitude alone gives

$$\left[\frac{d\sigma}{dE_p d\Omega_p}\right]' = \frac{16\pi}{9}\frac{P(E_p)}{q_1^2}$$
$$\times |\sin\delta_3(s_1) R_3^{(1/2)}(s_1, z_1)|^2. \tag{2.14}$$

We shall return to Eqs. (2.13) and (2.14) in later sections to determine why the coherent form produces the much sharper fsi peak.

There is a similar though more complicated coherence effect in the n-p fsi region of the neutron energy spectrum, from Eq. (2.6). More complicated because the n-p fsi occurs in both the $^3S_1$ and $^1S_0$ n-p spin states and hence all 11 terms in Eqs. (2.2)–(2.4) exhibit either n-p rescattering or are coherent with n-p rescattering. Taking the angular momentum decomposition of M_Q, M_{D1}, and M_{D2} with respect to, say, the n-p final-state relative momentum $\vec{q}_2$, we obtain

$$\frac{d\sigma}{dE_n d\Omega_n} = P(E_n)[\tfrac{2}{3}|M_Q^{(00)'}(s_2, z_2)|^2$$
$$+ \tfrac{1}{3}|M_{D1}^{(00)'}(s_2, z_2)|^2$$
$$+ \tfrac{1}{3}|M_{D2}^{(00)'}(s_2, z_2)|^2 + B_{np}(s_2, z_2)], \tag{2.15}$$

where $M_{D2}^{(00)'}(s_2, z_2)$ differes from $M_{D2}^{(00)}(s_1, z_1)$, and where $B_{np}(s_2, z_2)$ is a small incoherent background term which does not exhibit any fsi effect. Using the coupled integral equations of Eq. (2.1), Eq. (2.15) becomes, for the fsi part,

$$\left[\frac{d\sigma}{dE_n d\Omega_n}\right]_{\text{fsi}} = 4\pi P(E_n)\Big[\tfrac{2}{3}|F_1^{(1/2)}(s_2, z_2)|^2 + \tfrac{1}{3}|\tfrac{1}{2}F_1^{(1/2)}(s_2, z_2) + \tfrac{1}{2}F_2^{(1/2)}(s_2, z_2)|^2$$
$$+ \frac{1}{3}\Big|-\frac{\sqrt{3}}{2}F_1^{(1/2)}(s_2, z_2) + \frac{1}{2\sqrt{3}}F_2^{(1/2)}(s_2, z_2)\Big|^2\Big] \tag{2.16}$$

where the coherent fsi amplitudes are, including Eq. (2.12),

$$F_n^{(S)}(s, z) = \frac{e^{i\delta_n(s)}}{2iq}$$
$$\times \Delta[e^{i\delta_n(s)} R_n^{(S)}(s, z)]. \tag{2.17}$$

Equation (2.16) simplifies to the incoherent sum of three distinct n-p fsi terms,

$$\left[\frac{d\sigma}{dE_n d\Omega_n}\right]_{\text{fsi}} = 4\pi P(E_n)[\tfrac{2}{3}|F_1^{(3/2)}|^2 + \tfrac{1}{3}|F_1^{(1/2)}|^2 + \tfrac{1}{3}|F_2^{(1/2)}|^2], \tag{2.18}$$

where the first term is the $^3S_1$ n-p fsi in the three-particle quartet-spin channel, and the next two terms are the $^3S_1$ and $^1S_0$ n-p fsi, respectively, in the doublet-spin channel.

Equation (2.17) for the coherent fsi amplitude and the expressions in Eqs. (2.13) and (2.18) for the proton and neutron energy spectra in the fsi regions are the basic equations of the coherence effect in fsi in the n-d breakup reaction. Clearly similar results can be derived for other three-particle systems. The coherent fsi amplitudes carry the nucleon-nucleon phase factor $e^{i\delta_n(s)}$, and since we find that the remaining part of $F_n^{(S)}(s,z)$ varies rapidly in magnitude but slowly in phase [because $R_n^{(S)}(s,z)$ is not a real analytic function, this factor cannot be real], the phase factor $e^{i\delta_n(s)}$ describes the rapid phase variation of $F_n^{(S)}(s,z)$, as conjectured by Amado.[4] While the occurrence of this two-particle phase factor is a manifestation of the coherence effect, nevertheless it is the remaining factor of $F_n^{(S)}$ which describes the fsi peak structure. The simple and explicit form of this part is one of the main results reported here.[6] Amado's conjecture amounted to an extension of Watson's fsi theorem[8] to the case of three strongly interacting particles. When combined with analyticity assumptions, Watson's theorem in the two-particle case ($A+B-2+3$) implies[9] that the two-particle fsi amplitude can be factored into a part which varies slowly with s (the "production factor") and into a part (the "enhancement factor") which is rapidly varying, and which is approximately proportional to the 2-3 scattering amplitude.

Equation (2.17), however, shows that in the three-particle case we do not obtain a separation into enhancement and production factors. To appreciate this point we note that from Eq. (2.17) $F_n^{(S)}(s,z)$ satisfies the general discontinuity constraint

$$F_n^{(S)}(s+i\epsilon,z)-F_n^{(S)}(s-i\epsilon,z)=2iq\,F_n^{(S)}(s\pm i\epsilon,z)\times f_n(s\mp i\epsilon), \tag{2.19}$$

represented diagrammatically in Fig. 1, and which is familiar[10,11] as a subenergy normal threshold discontinuity, in S-matrix theory. Equation (2.19) is similar to the form of the unitarity constraint in two-particle multichannel reactions when we assume one particular channel dominates the on-shell intermediate states.[9] If we attempt a solution to Eq. (2.19) of the form

$$F(s,z)=f(s)G(s,z), \tag{2.20}$$

where $f(s)$ is the enhancement amplitude and $G(s,z)$ the production amplitude, then Eq. (2.19) implies $\Delta G(s,z)=0$, which is inconsistent with, for example, Eq. (2.9) for $F_3^{(1/2)}(s,z)$ which involves a term of the form $f(s)R(s,z)$, but for which $\Delta R(s,z)\neq 0$. Hence we are led to generalize Eq. (2.20) to the form

$$F(s,z)=f(s)R(s,z)+C(s,z), \tag{2.21}$$

where $C(s,z)$ describes additional processes coherent to the final rescattering. Equation (2.19) then implies that, if $\Delta C(s,z)=0$,

$$C(s,z)=\frac{1}{2iq}\Delta R(s,z),$$

and we obtain

$$F(s,z)=\frac{e^{i\delta(s)}}{2iq}\Delta[e^{i\delta(s)}R(s,z)], \tag{2.22}$$

in agreement with Eq. (2.17). Hence two-particle fsi amplitudes in three-particle systems are inherently more complicated than the usual Watson form, Eq. (2.20), which has been commonly used in three-particle reactions, and which implies that $|\sin\delta(s)|^2$ is the dominant term in the expression

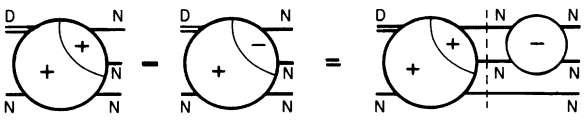

FIG. 1. The general fsi subenergy (upper signs indicate sheet) threshold discontinuity constraint on the fsi amplitude in a three-particle system (lower signs indicate three-particle total energy is in physical region).

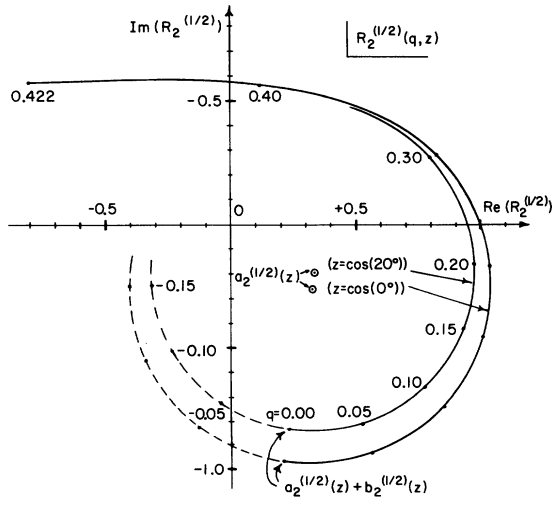

FIG. 2. The Argand plots of $R_2^{(1/2)}(q,z)$ for c.m. angles of 0 and 20° and for q in the physical breakup region. The dashed parts show analytic continuations to negative q values. The fsi region is $|q|<0.15$ fm^{-1} and $R_2^{(1/2)}=R_3^{(1/2)}$.

for the cross section. The complication arises from $\Delta R_n^{(S)} \neq 0$, which follows from the properties of the three-particle propagator in Eq. (2.1).

To exhibit the full content of Eqs. (2.13), (2.17), and (2.18) we need to know the detailed analytic form of $R_n^{(S)}(s, z)$, which we now determine.

III. AMPLITUDE PARAMETRIZATION

To study the form of $R_n^{(S)}(s, z)$ we have solved numerically the integral equations of Eq. (2.1) using, for simplicity, charge-independent rank-one Yamaguchi separable potentials and the contour-deformation method.[3] The potential parameters are given elsewhere,[3] but in particular $a_{nn} = -24$ fm and, because of assumed charge independence, $R_2^{(1/2)} = R_3^{(1/2)}$.

We find, from the numerical results, that in the forward direction and in the fsi region all the amplitudes $R_n^{(S)}(s, z)$ can be very accurately parametrized by the particularly simple form

$$R_n^{(S)}(s, z) = a_n^{(S)}(z) + b_n^{(S)}(z) \exp[i \phi_n^{(S)}(q, z)] , \tag{3.1}$$

where $a_n^{(S)}(z)$ and $b_n^{(S)}(z)$ are complex and the phase $\phi_n^{(S)}(q, z)$ is real and has the form

$$\phi_n^{(S)}(q, z) = 2r_n^{(S)}(z) q + \mu_n^{(S)}(z) q^3 . \tag{3.2}$$

Furthermore, if we iterate Eq. (2.1) we find that the single-plus-double scattering (spds) amplitudes $R_n^{(2,S)}(s, z)$ also have the parametrization of Eq. (3.2) in the same region.

To illustrate this parametrization we show in Fig. 2 the Argand plot of the amplitude $R_2^{(1/2)}(s, z)$ for the complete physical breakup region $0 \leq s \leq mE/\hbar^2$ and for scattering angles of 0 and 20° for the case $E_{n,\mathrm{lab}} = 14.4$ MeV. The fsi region is approximately $0 \leq s < 1$ MeV corresponding to $0 \leq q < 0.16\ \mathrm{fm}^{-1}$. In terms of the above parametrization $a_n^{(S)}(z)$ is the center of the circular section in Fig. 2 and $|b_n^{(S)}(z)|$ is the radius, while $\phi_n^{(S)}(q, z)$ determines the variation with q of $R_n^{(S)}(s, z)$ along the complex plot. In the fsi region this variation is almost linear in q, indicating that the contribution from $\mu_n^{(S)} q^3$ in Eq. (3.2) is small.

As well, we see from Eq. (2.17) that the coherent fsi amplitude requires the "physical" amplitude $R_n^{(S)}(s + i\epsilon, z)$ as well as the "unphysical" amplitude $R_n^{(S)}(s - i\epsilon, z)$. This amplitude is easily obtained from Eq. (3.1) by analytic continuation in q from positive to negative values, and $R_2^{(1/2)}(s - i\epsilon, z)$ is shown in Fig. 2 by the dashed plots.

The various parameter values for the forward direction ($z = +1$) are shown in Table I for both the exact solutions and the spds approximation, and we see that this approximation is in general very poor. This result is not unexpected, since for the doublet-spin channel the multiple-scattering series is divergent[12,13] at this energy.

There are some important and interesting features exhibited in Table I. First, in general $|b_n^{(S)}|$ is larger than $|a_n^{(S)}|$ for the exact solutions (at this particular total energy) and as a consequence, as we show in Sec. IV, of all these parameters, the shape of the fsi peak is determined mainly by the value of $r_n^{(S)}$. The variations in $\mu_n^{(S)}$ are unimportant since $2r_n^{(S)} q \gg \mu_n^{(S)} q^3$ in the fsi region. Hence the parameter of primary physical interest to fsi is $r_n^{(S)}$. An important feature of the $r_n^{(S)}$ values is that, in the doublet-spin channel, $r_1^{(1/2)}$ and $r_2^{(1/2)}$, for the exact solutions, differ from their mean value by less than 3%. The same effect is seen for the spds approximation. Hence, in all cases $r_n^{(S)}$ is, too a good approximation, independent of the nucleon-nucleon interaction label n, which also labels the coupled amplitudes, and thus $r_n^{(S)}(z)$ depends only on the three-particle channel-spin quantum number S, apart from z.

Thus $2r^{(1/2)} \simeq 9.91$ fm and $2r^{(3/2)} \simeq 7.59$ fm, which are, respectively, 25 and 10% larger than the $2r^{(S)}$ channel values from spds (7.85 and 6.80 fm), at $\theta = 0°$. This conclusion has important physical implications for our understanding of three-particle reactions, since these large variations

TABLE I. Forward-scattering parameter values [the $a_n^{(S)}$ and $b_n^{(S)}$ values differ from the definition in Eq. (3.1) by a normalization factor] for exact solution (E), single-plus-double scattering (D), and initial-state-interaction modified D (M).

S	n	$a_n^{(S)}$	$b_n^{(S)}$	$2r_n^{(S)}$ (fm)	$\mu_n^{(S)}$	
$\frac{3}{2}$	1	$1.135 + i1.810$	$0.192 + i3.475$	7.59	−34.7	(E)
		$0.199 + i2.680$	$-0.726 + i3.775$	6.80	−23.1	(D)
$\frac{1}{2}$	1	$1.054 + i1.696$	$2.453 + i3.317$	9.78	−34.5	(E)
		$3.911 + i3.164$	$3.269 + i6.006$	7.74	−31.7	(D)
$\frac{1}{2}$	2,3	$0.317 - i0.252$	$-0.112 - i0.717$	10.05	−21.3	(E)
		$-0.630 - i0.993$	$-0.243 - i1.274$	7.96	−31.6	(D)
		$0.111 - i0.273$	$-0.011 - i0.759$	9.28	−23.3	(M)

in $r^{(S)}$ have an interesting influence on the shape of the fsi peaks. Figure 3 shows the scattering-angle dependence of the various $r_n^{(S)}(z)$, which is seen to be small and approximately the same in all cases in the forward directions. Furthermore, from Fig. 3 we see that the difference $d^{(S)}$ between the exact value of $r_n^{(S)}(z)$ and the value obtained from spds is independent of z and n, for the range of angles shown in Fig. 3, and $d^{(S)}$ is shown by the vertical dashed lines in Fig. 3. The parameters $a_n^{(S)}$ and $b_n^{(S)}$ vary slowly with z.

We now consider the origin of the parametrization in Eq. (3.1), the physical significance of the main parameter $r^{(S)}$, and the interpretation of its large values for the exact solution. Since the spds approximation exhibits the parametrization, its origin should be most easily seen for this case, for which Eq. (2.11) becomes

$$\Delta R_n^{(2,S)}(s',z)=\frac{iq'}{2\pi}\sum_{n'=1}^{n_s}\chi_{nn'}^{(S)}\chi_{n'1}^{(S)}\int d\hat{q}'\left\langle \tfrac{1}{2}\vec{q}'+\tfrac{3}{4}\vec{k}'\left|t_{n'}\left(E-\tfrac{3}{4}(\tfrac{1}{2}\vec{q}'+\tfrac{3}{4}\vec{k}')^2\frac{\hbar^2}{m}\right)\right|\tfrac{1}{2}\vec{q}'-\tfrac{1}{4}\vec{k}'+\vec{k}\right\rangle$$
$$\times\phi(\vec{q}'+\tfrac{1}{2}(\vec{k}-\vec{k}'))\,. \qquad (3.3)$$

Here the scattering matrix is slowly varying for s' in the fsi region and the structure of the integrand is mainly determined by the deuteron wave function which has the general form

$$\phi(q)=\frac{\Gamma(q)}{q^2+\alpha_0^2}\,,$$

where $e=(\hbar^2/m)\alpha_0^2$ is the binding energy and, because the deuteron in weakly bound, the coordinate-space wave function is approximately

$$\psi(r)\simeq\frac{e^{-\alpha_0 r}}{r}\,,$$

where $\alpha_0^{-1}=4.3$ fm is a measure of the deuteron size. In the forward direction and in the fsi region when the momentum transfer $\vec{Q}=\frac{1}{2}(\vec{k}-\vec{k}')$ is small we find that Eq. (3.3) is well described by the form

$$\Delta R_n^{(2,S)}(s',z)\propto\sin(2r_0q'), \qquad (3.4)$$

where $r_0\simeq\frac{1}{4}\pi\alpha_0^{-1}$. This form is consistent with Eq. (3.1). Hence we interpret the parameter $r_n^{(S)}$ as a measure of the effective size of the deuteron, and since $r_n^{(S)}$ is very nearly independent of n, we see that the effective deuteron size is a property of the particular three-particle channel, rather than the individual amplitudes which are coupled in each channel.

It is evident from Eq. (3.3) that the form of $\Delta R_n^{(2,S)}$, as approximated in Eq. (3.4), is insensitive to the total three-particle energy E, except for very low energies when the energy dependence of the two-particle scattering matrix becomes important. Furthermore, the exact solution, which has the exponential parametrization at $E_{n,\mathrm{lab}}\simeq 14$ MeV, approaches the spds approximation at high energies, and thus the parametrization of the exact solution also is expected to be valid over a wide range of energies.

If we accept that $r^{(S)}$ is a measure of the effective deuteron size, in the channel with total spin S, and that in the $S=\frac{1}{2}$ channel $r^{(1/2)}$ is 25% larger than the corresponding value from spds, we are led to the conclusion that the deuteron is effectively dilated by 25% in this channel. We conjecture that this dilation can be interpreted as caused by the strong n-d initial-state interaction, which has been demonstrated to occur by Cahill and Sloan.[13] The initial-state interaction (isi) in the $S=\frac{3}{2}$ channel is apparently weaker, causing only an effective dilation of 10% compared with the spds ap-

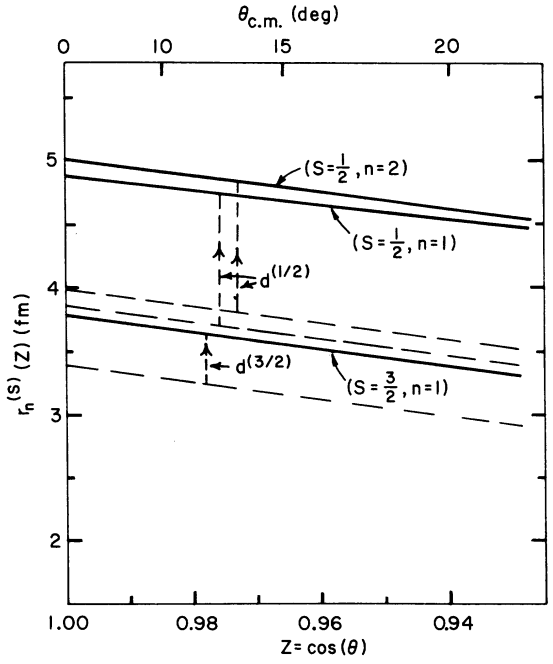

FIG. 3. The deuteron effective size parameter $r_n^{(S)}(z)$ (S is the three-particle spin and n labels coupled amplitudes) for various c.m. scattering angles θ. The dilation parameter $d^{(S)}$ is the difference between the exact and the single-plus-double scattering value (dashed) of $r_n^{(S)}$.

proximation. In this interpretation the constants $d^{(1/2)} = 1.03$ fm and $d^{(3/2)} = 0.40$ fm are then a measure of the deuteron dilation in the two uncoupled channels.

A dilation in coordinate space corresponds to a narrowing of the momentum distribution, and there is experimental evidence for this. To measure the momentum distribution of the deuteron components one performs a kinematically complete experiment and observes the so-called quasifree-scattering peak,[14,15] where the width of the peak is a measure of the momentum distribution of the nucleons in the deuteron. One observes[14,15] in fact, for $E_{n,\mathrm{lab}} \simeq 14$ MeV, that the width is narrower than that predicted by an unperturbed deuteron. Ideally the quasifree-scattering (qfs) process corresponds to scattering in which, in general, all but one of the target particles have their momentum unchanged, and where that one particle scatters the incident particle. However, clearly, when there is a strong isi between the incident particle and the bound-state target as a whole, which we expect at low energies in the n-d case, the qfs condition cannot be attained. It was shown[15] that incorporating explicitly[13] the isi into the usual qfs process one does obtain a narrowing of the qfs peak in agreement with experiment.

The concept of a certain definite target dilation during the breakup of that target clearly requires some consideration, particularly as we are working in a time-independent formalism. In a time-dependent formalism the bound-state target is of course undilated before the scattering event and the size is essentially undefined after the event when the bound-state components have separated. The above results, however, show that if we wish to reproduce certain significant features of the exact solution of the Faddeev equations by using the spds approximation, then in that approximation we should use an effective deuteron wave function which is more extended in coordinate space than the normal deuteron state. This dilation is some effective value between the initial and final values in a time-dependent view. This effective dilation is one important consequence of the higher-order multiple scattering events that are neglected in spds. An important feature of these higher-order multiple scatterings is that they contain implicitly an isi mechanism.[13] We find that an isi modification of spds increases the $r^{(1/2)}$ value by 16%.

In the next section we show how the important physical parameter $r^{(S)}$, which includes the isi process, strongly affects the fsi peak shapes.

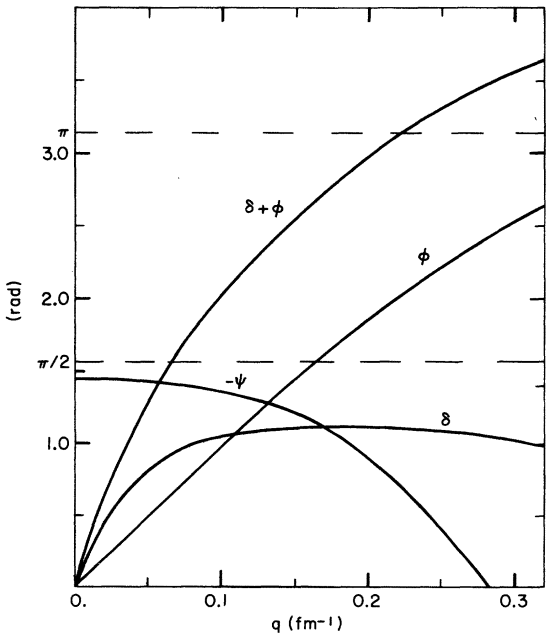

FIG. 4. Various phases, with δ the $^1S_0$ n-n phase shift for a scattering length of -24 fm and an effective range of 2.67 fm. Here ϕ is the phase of $R_2^{(1/2)}(q,z)$, in the forward direction ($\theta = 0°$), as defined in Eq. (3.1). The phase of the fsi amplitude is $\delta + \psi$, showing that the variation is described by δ in the fsi region. The rapidly changing phase $\delta + \phi$ essentially determines the n-n fsi peak shape, rather than δ alone as in the Watson-Migdal approximation.

IV. fsi CROSS SECTIONS

Combining the amplitude parametrization of Eq. (3.1) with the fsi coherence formalism, Eq. (2.17),

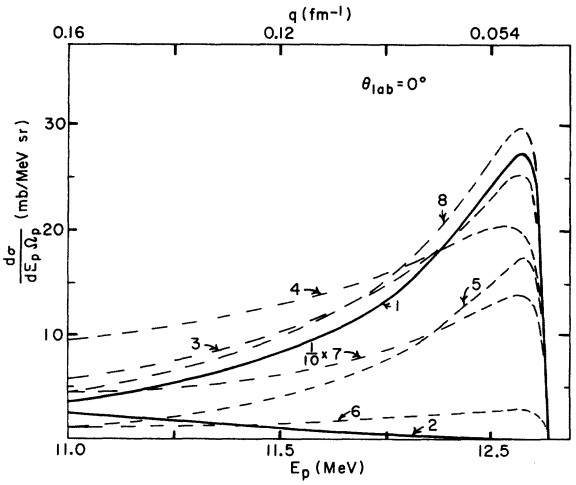

FIG. 5. Proton energy spectra for n-d breakup in the n-n fsi region at 14.4 MeV. The exact result is the sum of the pure fsi peak (curve 1) and the background contribution (curve 2). The remaining curves illustrate various aspects discussed in the text.

we obtain the explicit form of the final-state-interaction amplitude:

$$F_n^{(S)}(s,z)=\frac{e^{i\delta_n(s)}}{q}\times\{a_n^{(S)}(z)\sin\delta_n(s)+b_n^{(S)}(z)\sin[\delta_n(s)+\phi_n^{(S)}(q,z)]\}, \quad (4.1)$$

where $\phi_n^{(S)}(q,z)\simeq 2r^{(S)}q$. Then, in particular, the n-n fsi part of the proton spectrum is, from Eq. (2.13),

$$\left(\frac{d\sigma}{dE_p\,d\Omega_p}\right)_{\rm fsi}=\frac{4\pi}{9}\,\frac{P(E_p)}{q^2}\,|a_3^{(1/2)}\sin\delta_3(s)+b_3^{(1/2)}\times\sin[\delta_3(s)+2r^{(1/2)}q]|^2. \quad (4.2)$$

Similarly, from Eq. (2.18), we obtain the sum of three such cross-section expressions for the n-p fsi part of the neutron energy spectrum.

In Fig. 4 we show the n-n phase shift $\delta_3(s)$, the phase $\delta_3(s)+\phi_3^{(1/2)}(q,z)$, and the phase $\psi(q)$ of the complex amplitude in Eq. (4.2), and ψ is seen to be slowly varying in the fsi region. Hence the phase variation of the coherent fsi amplitude is given by the two-particle phase shift.[4]

The rapid variation of the phase $\delta_3(s)+\phi_3^{(1/2)}(q,z)$ from 0 through $\frac{1}{2}\pi$ as s increases from zero (and E_p decreases from maximum) combined with the observation that, because $|b_3^{(1/2)}/a_3^{(1/2)}|\simeq 1.8$, the second term in Eq. (4.2) dominates, explains simply why the observed n-n fsi peak in proton spectra from n-d breakup is very narrow (after unfolding energy resolution). From Eq. (4.2) [with $\phi_3^{(1/2)}$ given by Eq. (3.2)] and the parameter values in Table I we obtain the fsi peak shown in curve 1, Fig. 5. Combined with the small background term (curve 2 of Fig. 5) $P(E_p)B_{nn}(q,z)$, where we find[16]

$$B_{nn}(q,z)\simeq Bq^2$$

is a reasonable approximation for small q, we obtain exact agreement with the cross section obtained by numerical quadrature[3] of Eq. (2.5) with $|M|^2$ given by Eqs. (2.2)–(2.4).

To demonstrate the fsi coherence effect and the isi effect we show in Fig. 5, as well as the complete results, various other cross sections. The broad curve 4 of Fig. 5 is the cross section given by Eq. (2.14), which includes only those processes ending in n-n rescattering. The resulting considerably broadened curve demonstrates the effectiveness of the coherence mechanism. We see that the rescattering cross section, Eq. (2.14), depends only on the magnitude of $R_3^{(1/2)}$ which from Fig. 2 is slowly varying, whereas the correct fsi expression in Eq. (2.13) depends also on the phase, as defined in Eq. (3.1), of $R_3^{(1/2)}$ which is rapidly varying, with the rate of variation determined by twice the dilated deuteron size. We see from Eq. (4.2) that when we put $b_3^{(1/2)}=0$ we obtain the Watson-Migdal form of the fsi peak, which is shown by curve 6 of Fig. 5. The smallness of this cross section shows the unimportance of this Watson-Migdal term in Eq. (4.2) at this energy and that this term produces a very broad and incorrect cross section. On the other hand, when we put $a_3^{(1/2)}=0$ we obtain curve 5 of Fig. 5, which has a similar almost identical shape to the exact result. Thus the second term in Eq. (4.2) almost exclusively accounts for the shape of the n-n fsi peak at $E_{n,\rm lab}\simeq 14$ MeV. This shape is in turn determined by the n-n phase $\delta_3(s)$ (parametrized, say, by the scattering length a_{nn} and the effective range r_{nn}) and by the effective dilated deuteron size for the appropriate three-particle channel. To demonstrate the effect of the deuteron dilation and thus, as interpreted here, the isi, we show in curve 3 of Fig. 5 the broadened cross section obtained from Eq. (4.2) when $2r^{(1/2)}$ is reduced from 10.05 fm to the spds value of 7.96 fm, but with all other parameter values as given by the exact solution. For curve 7 of Fig. 5 we have used all the spds parameter values, and we obtain a cross section which is 5 times too large and very much broader than the exact result. This broadening is caused by the smaller undilated $r^{(1/2)}$ value and, from Table I, the fact that $|b_3^{(1/2)}|\simeq|a_3^{(1/2)}|$ in this case, causing the contribution from the Watson-Migdal-type term in Eq. (4.2) to be overestimated. Finally, in curve 8 of Fig. 5 we show the fsi cross section obtained by the approximation[13] which incorporates the isi into spds. We see that the isi greatly improves both the shape and magnitude of the spds approximation. From Table I we see that the amplitude parameters show that the isi has produced the expected deuteron dilation as well as the condition in the exact case at this energy, that the $b_n^{(S)}$ dominates the $a_n^{(S)}$ term.

The theory of fsi in three-particle systems developed here finds an interesting application in the reanalysis of some earlier proton spectra from n-d breakup. Simplifying Eq. (4.2) by neglecting the $a_3^{(1/2)}$, we obtain the essential contribution of the fsi amplitude to the cross section,

$$\frac{1}{q}\sin[\delta_3(s)+2r^{(1/2)}q]. \quad (4.3)$$

Bond[17] analyzed the proton spectra using the Watson form with an essentially *ad hoc* modification[18] to include a nucleon-nucleon boundary radius β

$\simeq 1.4$ fm,

$$\frac{1}{q}\sin[\delta_3(s)+\beta q]\,, \tag{4.4}$$

and obtained the best fit $a_{nn}^B = -26$ fm, at $E_{n,\,\mathrm{lab}} = 14$ MeV. From the similarity of Eqs. (4.3) and (4.4) and noting that

$$\delta_3(s) = -a_{nn}q + O(q^3),$$

we obtain an approximate correction relation between the true value of a_{nn} and the Bond value

$$a_{nn} \simeq a_{nn}^B - \beta + 2r^{(1/2)}\,. \tag{4.5}$$

Using the value of 10 fm for $2r^{(1/2)}$, Eq. (4.5) gives $a_{nn} \simeq -17$ fm, in excellent agreement with the charge-symmetry prediction of Noyes and Lipinski.[19]

In the Watson-Migdal approximation the n-n fsi shape is determined mainly by the value of $|a_{nn}|$, whereas the complete analysis here shows that the shape is actually determined, in an analogous manner, mainly by the value of $-a_{nn}+2r^{(1/2)}$. The difference of 10 fm at 14 MeV indicates very clearly why the use of the Watson-Migdal approximation and related approximations confused the answer to the question of charge independence or charge symmetry of nuclear forces. Furthermore, the dilation effect contributes 2 fm to $2r^{(1/2)}$ at 14 MeV, and more at lower energies. Thus the neglect of the dilation effect will give a_{nn} values intermediate between the charge-symmetry and charge-independence values.

Furthermore Bond[17] finds the anomaly that $|a_{nn}^B|$ as determined by Eq. (4.4) is strongly dependent on the three-particle energy of the experiment, and increases with decreasing energy, representing a shrinking of the n-n fsi peak. However, in terms of the present theory this energy dependence is easily understood and expected. From Eq. (4.5), with a_{nn} constant, Bond's observation implies that the deuteron dilation effect increases with decreasing three-body energy. That is, as the initial relative approach velocity of the neutron and deuteron is decreased the isi distortion becomes larger. Using Bond's values for a_{nn}^B, at various energies, in Eq. (4.5), we obtain the approximate energy dependence of the deuteron dilation, as shown in Fig. 6. Detailed experimental measurements of this dilation effect are required to properly determine the nature of this effect and the ability of theories to predict the dilation. A consequence of this energy dependence is that the observed qfs peak width should decrease with decreasing energy, compared to the width calculated from the undilated-deuteron wave-function momentum distribution. Care in the analysis of the qfs peak width will be required due to the differing dilations in the quartet- and doublet-spin channels.[20]

The coherence formalism and the dilation effect completely explain the sharpness of the n-n fsi peak in the proton spectra. However, the coherence effect can also broaden a fsi peak. From Eq. (4.1) we see that if the fsi pair has a positive scattering length, say the $^3S_1$ n-p pair, then the variations in δ_n and $\phi_n^{(S)}$ will tend to cancel rather than reinforce, as in the $^1S_0$ n-n case. Hence the fsi theory allows the sign of the scattering length to be determined.

For single-particle spectra Eq. (4.2) implies that the Watson-Migdal fsi approximation is only valid for those three-body energies for which $|a_n^{(s)}| \gg |b_n^{(s)}|$, and this condition is certainly not satisfied in a range of energies about 14 MeV. However, it has been claimed[21,22] that in kinematically complete experiments the Watson-Migdal expression is a good approximation.[23]

In the terms of the present analysis we can establish criteria for the applicability of the Watson-Migdal form in this case also. In a kinematically complete experiment in which we observe, for example, the n-n fsi, it is possible to choose the geometry so that only the n-n rescattering term in Eq. (2.4) is important, unlike the situation in the corresponding incomplete experiment where the n-p qfs interferes with the n-n rescattering. Then from Eqs. (2.4), (2.10), and (3.2) the differential-cross-section shape in the n-n rescattering region is determined approximately by, except for

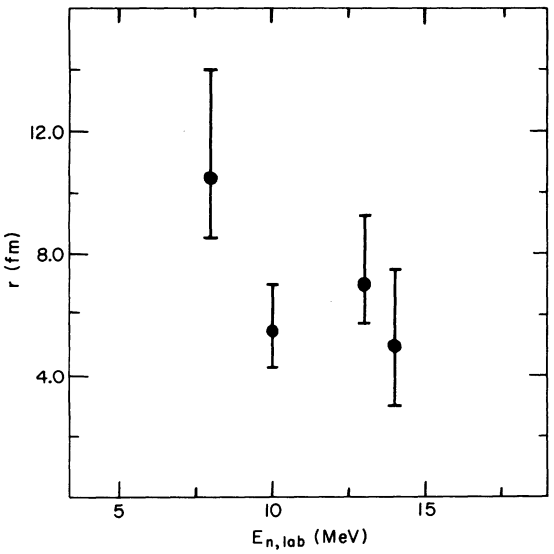

FIG. 6. The three-particle energy dependence of the deuteron effective size parameter r in the n-d doublet-spin channel, as determined approximately from Eq. (4.5). The error bars indicate only error analysis in data used (Ref. 17). Energy axis starts at n-d breakup threshold.

the phase-space factor,

$$\frac{1}{q^2}\sin^2\delta_3(s)\left|a_3^{(1/2)}(z)+b_3^{(1/2)}(z)\exp(2ir^{(1/2)}q)\right|^2, \tag{4.6}$$

and the Watson-Migdal form appears if either

$$|a_3^{(1/2)}| \gg |b_3^{(1/2)}|$$

or

$$|a_3^{(1/2)}| \ll |b_3^{(1/2)}| .$$

From Fig. 2 we see that in fact the amplitude in Eq. (4.6) is varying only slowly in magnitude, and to this extent the Watson-Migdal form is applicable at 14 MeV. Again, however, we see that the deviations depend on the deuteron size. The strongest deviations from the Watson-Migdal form will occur, for complete experiments, in the intermediate case of

$$|a_3^{(1/2)}| \simeq |b_3^{(1/2)}| .$$

It is evident that we have finally obtained a clearer insight into the theoretical aspects of final-state interactions in three-particle systems, particularly in kinematically incomplete experimental configurations. The final-state-interaction theory has recently been applied to the analysis of new n-n fsi data from n-d breakup.[16] A similar reanalysis of older experiments should go a long way in removing the many discrepancies in the previously extracted n-n scattering length values. Both the approximate reanalysis above of one experiment and the new analysis[16] imply charge symmetry of nuclear forces. The fsi theory developed in detail here for the n-d case can be formulated for other three-particle and quasi-three-particle systems.

---

*Research supported by the Australian Research Grants Committee.

[1]L. D. Faddeev, Zh. Eksp. Teor. Fiz. 39, 1459 (1960) [transl.: Sov. Phys.-JETP 12, 1014 (1967)].
[2]R. Aaron and R. D. Amado, Phys. Rev. 150, 857 (1966).
[3]R. T. Cahill and I. H. Sloan, Nucl. Phys. A165, 161 (1971).
[4]R. D. Amado, Phys. Rev. 158, 1414 (1967).
[5]I. J. R. Aitchison and C. Kacser, Phys. Rev. 173, 1700 (1968).
[6]R. T. Cahill, Flinders Report No. R-75, 1973 (unpublished).
[7]K. L. Kowalski, Phys. Rev. Lett. 15, 798 (1966).
[8]K. M. Watson, Phys. Rev. 88, 1163 (1952).
[9]J. Gillespie, *Final State Interactions* (Holden-Day, San Francisco, California, 1964).
[10]J. S. Ball, W. R. Frazer, and M. Nauenberg, Phys. Rev. 128, 478 (1962).
[11]R. J. Eden, P. V. Landshoff, D. I. Olive, and J. C. Polkinghorne, *The Analytic S-matrix* (Cambridge U. P., Cambridge, England, 1966).
[12]I. H. Sloan, Phys. Rev. 185, 1361 (1969).
[13]R. T. Cahill and I. H. Sloan, Nucl. Phys. A194, 589 (1972).
[14]I. Slaus, J. W. Sunier, G. Thompson, J. C. Young, J. W. Verba, D. J. Margaziotis, P. Doherty, and R. T. Cahill, Phys. Rev. Lett. 26, 789 (1971).
[15]D. J. Margaziotis, J. C. Young, I. Slaus, G. Anzelon, F. P. Brady, and R. T. Cahill, Phys. Lett. 37B, 263 (1971).
[16]S. Shirato, K. Saitoh, N. Koori, and R. T. Cahill, Nucl. Phys. (to be published).
[17]A. Bond, Nucl. Phys. A120, 183 (1968).
[18]R. J. N. Phillips, Nucl. Phys. 53, 650 (1964).
[19]H. P. Noyes and H. M. Lipinski, Phys. Rev. C 4, 995 (1971).
[20]R. T. Cahill, Nucl. Phys. A185, 236 (1972).
[21]W. Ebenhöh, in *Few Particle Problems in the Nuclear Interaction*, edited by I. Šlaus, S. A. Moszkowski, R. P. Haddock, and W. T. H. Van Oers (North-Holland, Amsterdam, 1972), p. 325.
[22]W. Breunlich, S. Tagesen, W. Bertl, and A. Chaloupka, in *Few Particle Problems in the Nuclear Interaction* (see Ref. 21), p. 100.
[23]A. B. Migdal, Zh. Eksp. Teor. Fiz. 28, 3 (1955) [transl.: Sov. Phys.-JETP 1, 2 (1955)].